

## Depletion-Induced Encapsulation by Dumbbell-Shaped Patchy Colloids Stabilize Microspheres against Aggregation

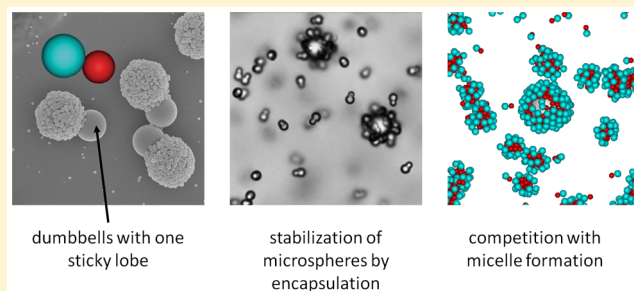
Joost R. Wolters,<sup>†,§</sup> Joanne E. Verweij,<sup>†,§</sup> Guido Avvisati,<sup>‡</sup> Marjolein Dijkstra,<sup>‡</sup> and Willem K. Kegel\*,<sup>†</sup>

<sup>†</sup>Van 't Hoff Laboratory for Physical and Colloid Chemistry, Debye Institute for Nanomaterials Science, Utrecht University, Utrecht 3584 CH, The Netherlands

<sup>‡</sup>Soft Condensed Matter, Debye Institute for Nanomaterials Science, Utrecht University, Utrecht 3484 CC, The Netherlands

### Supporting Information

**ABSTRACT:** In this paper, we demonstrate the stabilization of polystyrene microspheres by encapsulating them with dumbbell-shaped colloids with a sticky and a nonsticky lobe. Upon adding a depletant, an effective short ranged attraction is induced between the microspheres and the smaller, smooth lobes of the dumbbells, making those specifically sticky, whereas the interaction with the larger lobes of the dumbbells is considerably less attractive due to their rough surface, which reduces the overlap volume and leaves them nonsticky. The encapsulation of the microspheres by these rough-smooth patchy dumbbells is investigated using a combination of experiments and computer simulations, both resulting in partial coverage of the template particles. For larger microspheres, the depletion attraction is stronger, resulting in a larger fraction of dumbbells that are attached with both lobes to the surface of microspheres. We thus find a template curvature dependent orientation of the dumbbells. In the Monte Carlo simulations, the introduction of such a small, curvature dependent attraction between the rough lobes of the dumbbells resulted in an increased coverage. However, kinetic constraints imposed by the dumbbell geometry seem to prevent optimal packing of the dumbbells on the template particles under all investigated conditions in experiments and simulations. Despite the incomplete coverage, the encapsulation by dumbbell particles does prevent aggregation of the microspheres, thus acting as a colloid-sized steric stabilizer.



## INTRODUCTION

In nature, many functional structures are formed by self-assembly from smaller, basic building blocks. Examples are the formation of micelles from surfactant molecules or virus capsids from individual capsomers. While surfactants and some capsomers are able to self-assemble into larger, functional structures on their own, their self-assembly can also be assisted by a template which usually provides functionality of the resulting structure. Virus capsids generally form around the genetic material they are supposed to protect, while surfactants can assemble on the surface of an oil droplet, stabilizing it against coalescence. Understanding these processes and being able to mimic them on a colloidal scale enables the formation of new, complex, functional materials by self-assembly of colloidal building blocks.

In this paper, a system of patchy dumbbell-shaped colloids consisting of a smaller sticky and a larger nonsticky lobe are used as model surfactants or capsomers. These dumbbells are known to self-assemble into micelle-like clusters on their own<sup>1</sup> and are now used in a templated self-assembly experiment, using a large, smooth microsphere as a template. This packing of cone-shaped dumbbells on a spherical object is intuitively reminiscent of the stabilization of an oil droplet by surfactant molecules or the assembly of a virus capsid. Patchy model systems for the formation of empty virus capsids<sup>2–5</sup> and the

assembly of virus capsids around a core particle<sup>6</sup> have been studied in theory and simulations. Recently, Munaò et al.<sup>7</sup> presented simulations of the encapsulation of spherical particles by Janus dumbbells. However, this paper provides a first experimental investigation of encapsulating a spherical template particle by patchy colloidal particles.

The patchy dumbbell-shaped colloids used in this experiment are similar to the rough-smooth dumbbells used previously by Kraft et al.<sup>1</sup> Upon addition of the proper depletant, the smooth lobes of these particles become sticky, while the rough lobes remain nonsticky, leading to the formation of finite-sized micelle-like clusters. Larger, smooth microspheres are introduced in this system as a template. The overlap volume created when two particles come close enough for their depletion zones to overlap is larger for a microsphere and the smooth lobe of a dumbbell than for two dumbbells, resulting in a stronger depletion attraction. This facilitates microsphere encapsulation at relatively weak dumbbell–dumbbell attraction. By combining optical microscopy observations of this system with Monte Carlo simulations, we investigate the degree of coverage and the orientation of dumbbells on the microsphere surface as a

Received: January 9, 2017

Revised: March 1, 2017

Published: March 8, 2017

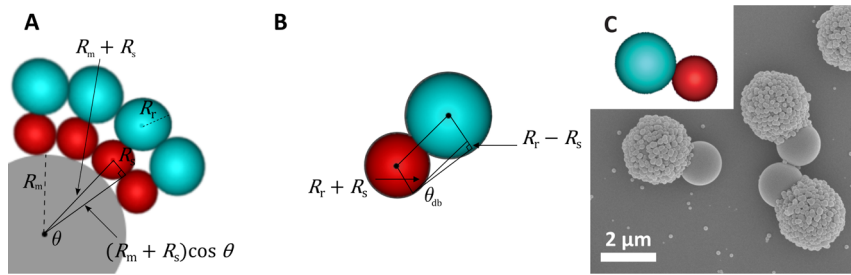


**Figure 1.** (A) Schematic representation of the geometric packing of dumbbells on a larger sphere with radius  $R_m$ , showing the angle  $\theta$  that defines the optimal packing according to eqs 1 and 2. (B) Close-up of a single dumbbell. The angle  $\theta_{db}$  defined by the size difference between the rough and smooth lobe constrains the optimal packing of dumbbells on a large sphere and defines the radius of the large sphere  $R_{ideal}$  for which the dumbbell packing is optimal. (C) SEM image of the rough-smooth dumbbells used in this paper, with a schematic representation of such a dumbbell as an inset.

function of microsphere size and interaction strength. By assessing bond lifetimes in microscopy experiments, comparing the degree of micelle formation and microsphere encapsulation and applying a kinetic model, we rationalize why the dumbbells do not completely cover the template microspheres in the final structure. These results are compared to a control experiment with spheres instead of dumbbells. Furthermore, the shielding effect of a cover of dumbbell-shaped particles as a stabilizer against microsphere aggregation is experimentally investigated.

## EXPERIMENTAL SECTION

**Particle Synthesis.** The spherical polystyrene particles used in the experiments we describe in this paper were synthesized by dispersion polymerization using a modified synthesis protocol of Hong et al.<sup>8</sup> These particles were subsequently swollen to a larger size and cross-linked using seeded emulsion polymerization to form the template microspheres.

The rough-smooth dumbbells were prepared using a seeded emulsion polymerization process described previously by Kim et al.<sup>9</sup> and Kraft et al.<sup>1</sup> In this method, non-cross-linked spherical polystyrene particles are first cross-linked and made rough by seeded emulsion polymerization. These rough, cross-linked particles are then used as seeds in a similar process to form a smooth protrusion. Both the microspheres and dumbbell particles have their surface coated with poly(vinyl alcohol) (PVA,  $M_w = 85\text{--}124 \text{ kg mol}^{-1}$ ) as steric stabilization against van der Waals forces. A more detailed description of the particle synthesis is provided in the Supporting Information.

**Sample Preparation.** In order to study the templated self-assembly of rough-smooth dumbbell particles, samples with varying particle and depletant (dextran) concentrations were prepared. Capillaries ( $0.10 \text{ mm} \times 2.00 \text{ mm}$  internal dimensions, Vitrotubes W5010-050) were filled with these dispersions. To prevent interaction with the capillary walls, these were first coated with dextran, as done in previous studies.<sup>1,10,11</sup>

Sample mixtures were made with different particle and depletant concentrations. Typically, aliquots of a 10% v/v dispersion of dumbbells and a 3% v/v dispersion of microspheres were mixed with aqueous solutions of  $116 \text{ g L}^{-1}$  dextran (from Leuconostoc spp.,  $M_w \approx 500 \text{ kg mol}^{-1}$ , Sigma-Aldrich), 77 mM sodium azide (99% extra pure, Merck), and 1 M NaCl.  $D_2O$  was added to a volume fraction of 0.46. This resulted in samples with a typical dumbbell volume fraction of  $\phi_p = 1\%$  and a microsphere volume fraction of  $\phi_m = 0.03\%$ , containing 30 mM of salt and a depletant volume fraction  $\phi_d$  of 0.40 to 0.57, where  $\phi_d = \rho/\rho_{overlap}$ , the depletant concentration as fraction of the overlap concentration ( $29 \text{ g L}^{-1}$ , as calculated from the hydrodynamic radius and molar mass of the dextran). The coated capillaries were filled with the sample mixtures and glued to object slides using UV-curable glue (Norland Optical Adhesive 81).  $D_2O$  was added to a volume fraction of 0.46 to reduce the density difference between particles and medium, greatly reducing the effect of particle sedimentation. Despite this density matching, particles still sedimented

at a slow rate. To compensate for this, samples were stored on a tube roller, tumbling them gently (30 rpm) to keep them suspended between measurements. Only samples without air bubbles were kept for analysis to make sure that shear has no effect on the system.

**Analysis.** The dimensions of the rough-smooth dumbbells and spherical particles were determined by analyzing TEM images taken using a FEI Tecnai 10 transmission electron microscope. The size distribution of the microspheres was obtained from the analysis of optical microscopy images using the program *ImageJ*.<sup>12,13</sup> The surface roughness of the microspheres and dumbbells was investigated using a scanning electron microscope (SEM XL FEG 30, Philips). A Malvern ZetaSizer Nano-ZS was used to measure both the polymer size of the depletant with dynamic light scattering (DLS) and the zeta potential of both the microspheres and dumbbells using laser doppler electrophoresis. Encapsulation of the microspheres with dumbbell particles was studied using a Nikon Eclipse Ti optical microscope with a Nikon Plan Fluor air objective (NA = 0.75, 40 $\times$  magnification). A Nikon Apo TIRF oil immersion objective (NA = 1.49, 100 $\times$  magnification) was used to study the encapsulation of microspheres by the smaller spherical particles. All images were acquired with an additional 1.5 $\times$  magnification. Image acquisition was performed using a Hamamatsu Digital Camera ORCA-Flash4.0 C11440 and the NIS-Elements Imaging Software.

**Packing Dumbbells on a Sphere.** When covering a larger spherical particle with smaller spheres, the maximum number of smaller spheres that can cover the surface of the large sphere depends on the size ratio between the spheres.<sup>14</sup> Small spheres with radius  $R_s$  packed on a larger sphere with radius  $R_m$  have their centers defined on the surface of a sphere with radius  $R_m + R_s$ . However, the contacts with the other small spheres are positioned on a sphere with a radius of  $(R_m + R_s) \cos(\theta)$ ,<sup>15</sup> as depicted schematically for the dumbbells in Figure 1A. The angle

$$\theta = \arcsin\left(\frac{R_s}{R_m + R_s}\right) \quad (1)$$

defines roughly how many small spheres can cover a larger sphere. For dumbbell-shaped particles, optimal packing is achieved when both the small and the large lobes of the dumbbells are in contact, resulting in both the highest concentration of dumbbells on the surface and the maximum number of contacts between the dumbbells. This means that the angle  $\theta$  at optimal packing is defined by the radii of both lobes as (Figure 1B):

$$\theta_{db} = \arcsin\left(\frac{R_r - R_s}{R_r + R_s}\right) \quad (2)$$

This optimal angle  $\theta_{db}$ , defined by the geometry of the dumbbell, in turn defines the radius  $R_{ideal}$  of the larger microsphere that can ideally be packed by dumbbells of this geometry via:

$$R_{ideal} = \frac{R_s}{\sin \theta_{db}} - R_s \quad (3)$$

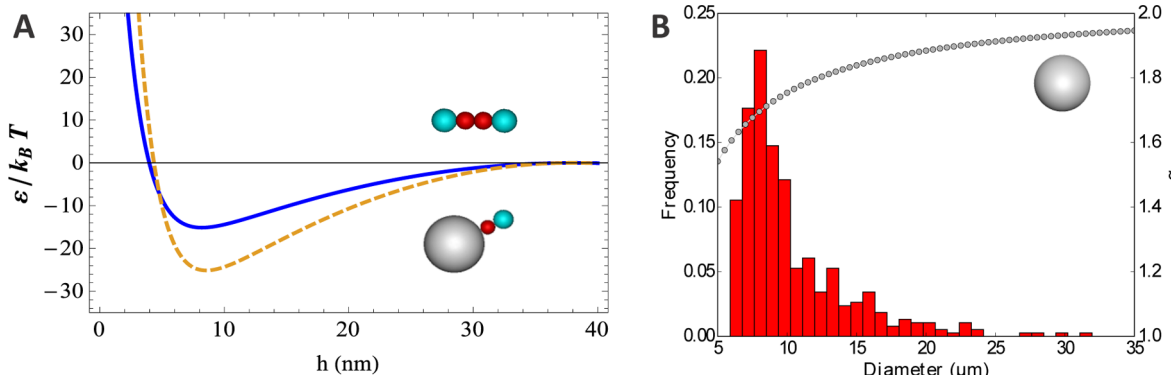


**Figure 2.** (A) Interaction potential in  $k_B T$  as a function of the inter particle (surface-to-surface) distance  $h$  between the smooth lobes of two dumbbells (solid blue line) and the stronger attraction between the smooth lobe of a dumbbell and a microsphere surface (dashed yellow line). These plots were constructed using the experimentally obtained dimensions and surface potential of the dumbbells and assuming the ideal radius  $R_{\text{ideal}} = 4.83 \mu\text{m}$  for the microspheres in a dispersion with  $I(M) = 30 \text{ mM}$  and depletant volume fraction  $\phi_d = 0.43$ . (B) The broad size distribution of the microsphere template particles used, with an average diameter of  $10 \pm 4 \mu\text{m}$  and a high fraction of particles with a diameter close to the ideal diameter of  $9.67 \mu\text{m}$ . The gray markers indicate the factor  $\alpha$  (right vertical axis) by which  $\varepsilon$  between a dumbbell and a microsphere of this size is larger than the dumbbell-dumbbell interaction (the ratio between the two potential minima in A) as calculated from eqs S1–S7 in the Supporting Information, based on the difference in overlap volume and surface potential.

The packing in this arrangement is optimal not only because it allows for a maximum number of dumbbells to attach to the larger sphere but also because it maximizes the number of contacts between the attractive lobes of the dumbbells on the surface.

**Interaction Potential.** The interaction potential between the smooth lobes of the dumbbells and the microspheres is determined by a depletion attraction  $u_{\text{depl}}$ , depending on the overlap volume  $V_{\text{overlap}}$  between the particles and the depletant concentration. This attraction is balanced by an electrostatic repulsion  $u_{\text{el}}$  depending on the surface potential of the particles and screened by the salt concentration. The net interaction potential  $u_{\text{depl}} + u_{\text{el}}$  can be tuned in experiments by changing either the salt or depletant concentration. Since  $V_{\text{overlap}}$  increases with the radii of the particles and the template microspheres are much larger than the smooth lobes of the dumbbells, the smooth lobes of the dumbbells bind more strongly to the template microspheres than to each other. Figure 2A shows the net interaction potentials between the smooth lobes of two dumbbells (solid blue line) and the stronger interaction between the smooth lobe of a dumbbell and a microsphere (dashed yellow line) under typical experimental conditions. Based on the size of the roughness ( $r \approx 76 \text{ nm}$ ) on the rough lobes of the dumbbells and the much smaller radius of gyration ( $r_g$ ) of the depletant, a significantly lower  $V_{\text{overlap}}$  and consequently weaker interaction is expected with the rough lobes of the particles.<sup>1,11</sup> More details on the calculation of the interaction potentials are provided in the Supporting Information.

Furthermore, the net interaction is very short ranged ( $\sim 0.02 \times$  the particle diameter) due to both the small size of the depletant ( $r_g = 19 \pm 6 \text{ nm}$ ) and the short Debye length ( $\kappa^{-1} \approx 2 \text{ nm}$ ) compared to the size of the particles ( $> 1 \mu\text{m}$ ). In the case of such “sticky” particles, with an interaction range of  $2r_g$  and a strength of  $\varepsilon$  (the depth of the potential well) the exact shape of the interaction potential is known to have little effect on the behavior of the system.<sup>11,16,17</sup> In simulations, this potential can therefore be expressed as a square-well potential with the width  $\Delta = 2r_g$  and depth  $\varepsilon$ .

**Simulation Model.** Alongside the experiments, Monte Carlo (MC) simulations in the canonical ensemble (NVT) were also used to study the packing of dumbbells on a microsphere. In these simulations, a single static microsphere was placed in the center of a simulation box containing 800 dumbbells. The dumbbells were modeled by tangent hard spheres representing the smooth (sticky) and rough (nonsticky) lobe of the dumbbell. The diameter of the smooth lobe  $\sigma_s = 2R_s$  and rough lobe  $\sigma_r = 2R_r$  were chosen such that the diameter ratio  $q = \sigma_r/\sigma_s$  matches that of the dumbbells used in experiments. Simulations were performed for  $1 \times 10^6$  MC cycles. Hereby each MC cycle is defined as 1200 particle moves which can either be particle rotations or

translations. During the first  $2.5 \times 10^5$  MC cycles values for displacements and rotations are adjusted to obtain an acceptance rate of 30% for the proposed moves. Most of the parameters in the model, like number density, were fixed to match the experimental system as closely as possible. The interaction energy  $\varepsilon/k_B T$  (with  $k_B$  being the Boltzmann constant and  $T$  the temperature) between the dumbbells was varied to study how this affects the packing of dumbbells on the microsphere.

The basic interaction between two smooth lobes  $i$  and  $j$  was described by a hard-sphere square-well potential:

$$u^{\text{SW}}(r_{ij}) = \begin{cases} \infty & \text{if } r_{ij} < \sigma_s \\ \varepsilon & \text{if } \sigma_s \leq r_{ij} < \sigma_s + \Delta \\ 0 & \text{if } r_{ij} \geq \sigma_s + \Delta \end{cases} \quad (4)$$

where  $r_{ij}$  is the center-to-center distance between the smooth lobes,  $\varepsilon < 0$  denotes the depth of the well, and  $\Delta$  is the range of the interaction.

The interaction between a smooth lobe  $i$  and a microsphere  $m$  was described by a similar square-well potential. However, in this case the depth of the well is represented by  $\alpha\varepsilon$ . Factor  $\alpha$  represents the factor with which the interaction energy is increased due to the larger overlap volume between a dumbbell and a microsphere. This factor  $\alpha$  increases with the microsphere radius as shown in Figure 2B.

While the surface of the rough lobes on the dumbbells drastically lowers  $V_{\text{overlap}}$ , these lobes can still become slightly attractive, especially at higher depletant concentrations. To represent this in the simulations, an attraction between two rough lobes or the rough and smooth lobe of different dumbbells of  $\gamma\varepsilon$  was introduced, with  $0 < \gamma < 1$ . At  $\gamma = 0$ , the rough lobes simply behave as hard objects, while at larger values of  $\gamma$ , a (small) attraction is introduced. Correspondingly, the square-well interaction between rough lobes and the microsphere has a well depth of  $\alpha\gamma\varepsilon$ . In the simulations, the value of  $\gamma$  is systematically varied to study the effect of rough–rough attraction on the coverage of the microsphere and the orientation of the dumbbells on its surface.

The simulation results of the bound dumbbells were analyzed using a binding criterion. A dumbbell was considered to be bound to the microsphere when the outer distance between either the smooth or rough lobe and the microsphere was less than the square-well interaction range  $\Delta$ . Consistently, without interaction between the rough lobes of the dumbbells, the binding criterion does not consider rough lobes inside the square-well interaction range to be bound to the microsphere. Occasionally, a dumbbell would attach to the first layer of dumbbells already bound to the microsphere. Dumbbells in this

second layer are considered bound as well according to the previously mentioned binding criteria.

## RESULTS AND DISCUSSION

In this section we first present the properties (dimensions and surface potential) of the synthesized particles in relation to the expected encapsulation behavior. Next, the depletant concentration is tuned to find the interaction potential most favorable for encapsulation. We subsequently describe the encapsulation structures observed under these conditions and compare these to the results from simulations, as well as the encapsulation of microspheres by spherical colloids. Finally, we describe how the encapsulation by rough-smooth dumbbells prevents the aggregation of microspheres and rationalizes the degree of microsphere coverage in competition with the formation of micelle-like structures using a kinetic model.

**Particle Properties.** The properties of the template microspheres and the dumbbell-shaped and spherical particles used in this paper are presented in Table 1. The zeta potential

**Table 1. Overview of the Properties of the Colloidal Particles Used in This Paper<sup>a</sup>**

|                       | $R_s$ ( $\mu\text{m}$ ) | $R_r$ ( $\mu\text{m}$ ) | zeta potential (mV) |
|-----------------------|-------------------------|-------------------------|---------------------|
| dumbbells             | $0.81 \pm 0.04$         | $1.08 \pm 0.05$         | $-16 \pm 5$         |
| small spheres         | $0.488 \pm 0.013$       |                         | $-24 \pm 5$         |
| template microspheres | $5 \pm 2$               |                         | $-19 \pm 4$         |

<sup>a</sup>For the spherical particles,  $R_s$  simply denotes the radius.

of the dumbbell particles is derived from their electrophoretic mobility assuming spherical particles and is therefore only an estimate of the actual surface potential ( $\Psi$ ) on the smooth lobes of the dumbbells that contributes to the net attractive potential.

A SEM image of these dumbbells is shown in Figure 1C, with a schematic representation of these dumbbells as an inset. Based on their dimensions, these dumbbells have an angle at optimal packing of  $\theta_{db} = 8.22^\circ$  (eq 2). This angle is exactly met when the dumbbells are packed on a sphere with radius  $R_{ideal} = 4.83 \mu\text{m}$  (eq 3) and is in between the angles corresponding to icosahedrally symmetric packings of 132 and 140 particles on a sphere.<sup>18</sup> Therefore, an optimal packing is in this case expected to consist of 132 to 140 dumbbells.

The microspheres used as templates in the encapsulation experiments have a broad size distribution with an average close to the diameter of a microsphere that can ideally be packed by the used dumbbells ( $2 \times R_{ideal} = 9.67 \mu\text{m}$ ). This size distribution of the microspheres is provided in Figure 2B. The use of template particles in the size range of the dumbbells is less ideal as the attraction between template and dumbbell is lower and the obtained structure is harder to investigate.

**Encapsulation Conditions.** We performed encapsulation experiments in an aqueous dispersion with a typical dumbbell volume fraction of  $\phi_p = 1\%$  and a microsphere volume fraction of  $\phi_m = 0.03\%$ . Keeping the concentration of microspheres very dilute ensured an excess of dumbbells per microsphere ( $\gg 140$  per microsphere). While keeping the salt concentration constant at 30 mM, the depletant concentration was changed to tune the interaction potential. As the overlap volume between a microsphere and dumbbell is higher compared to the overlap volume between two dumbbells, the attraction is

stronger. This suggests there is a regime of depletant concentrations where the attraction is strong enough to encapsulate microspheres with dumbbells, whereas the depletion attraction between dumbbells is not strong enough to form clusters.

At low depletant concentrations ( $\phi_d < 0.40$ , Figure 3A) dumbbells and microspheres are free in solution. Occasionally, small dumbbell clusters or dumbbells attached to a microsphere are observed. Increasing the polymer concentration leads to the attachment of more dumbbells to the microspheres at  $\phi_d = 0.43$ . Dumbbell clusters are still very small, indicating a small attraction between the dumbbells. This situation is shown in Figure 3B. At this concentration, the microspheres are not homogeneously covered with dumbbells. Upon increasing the depletant concentration further, the coverage of the microspheres does not increase significantly, but the dumbbell-dumbbell interaction becomes sufficiently strong to form clusters of dumbbells ( $\phi_d = 0.45$ , Figure 3C). At higher depletant concentrations, specificity of the dumbbells is lost as the rough lobes also become attractive. As a demonstration of this effect, Figure 3D shows random, nonspecific aggregates of dumbbells and microspheres at  $\phi_d = 0.48$ . We observed that the crossover from free dumbbells and microspheres in solution, toward random aggregation occurs in a very narrow range of depletant concentrations. At  $\phi_d = 0.43$ , we observed encapsulation of microspheres by specifically attached dumbbells, with hardly any cluster formation of (non)specifically binding dumbbells. Therefore, these conditions were chosen to investigate the encapsulation behavior in detail, as described in the next section.

**Encapsulation Structure.** We left the samples to equilibrate for 3 days, after which we hardly observed any changes in the structure of the encapsulated microspheres in the capillaries. We therefore considered the then observed encapsulated microspheres to be the stabilized final structure of the system. In addition, both microspheres and dumbbells were homogeneously suspended throughout the capillary, indicating that gravity or the capillary walls had not influenced the observed structures. The system consists primarily of separate microspheres with only rarely observed aggregates of multiple microspheres. All microspheres were covered with an incomplete monolayer of dumbbell particles (Figures 3B and 4).

Upon investigating the encapsulation of different sizes of microspheres, we observed a strong dependence on microsphere size. Moderately sized microspheres, with a diameter of 8–13  $\mu\text{m}$ , are partly encapsulated by dumbbells attached to the microsphere by their smooth lobe, leaving the rough lobe free to move and allow the dumbbells to change their orientation with respect to the microsphere. Dumbbells were found to predominantly orient perpendicular to the microsphere surface.

For bigger microspheres, with a diameter larger than 25  $\mu\text{m}$ , dumbbells appear to be positioned flat on the surface, bound by an additional bond between the microsphere and the rough lobe of the dumbbell. However, also in this orientation we observed particle mobility, showing a higher mobility of the rough lobe. This indicates that the rough lobe is indeed less tightly bound than the smooth one. Figure 4 shows typical examples of small and large microspheres with the dumbbell particles respectively oriented perpendicular and parallel to the microsphere surface. In neither case we found complete coverage of the microspheres with dumbbell particles.

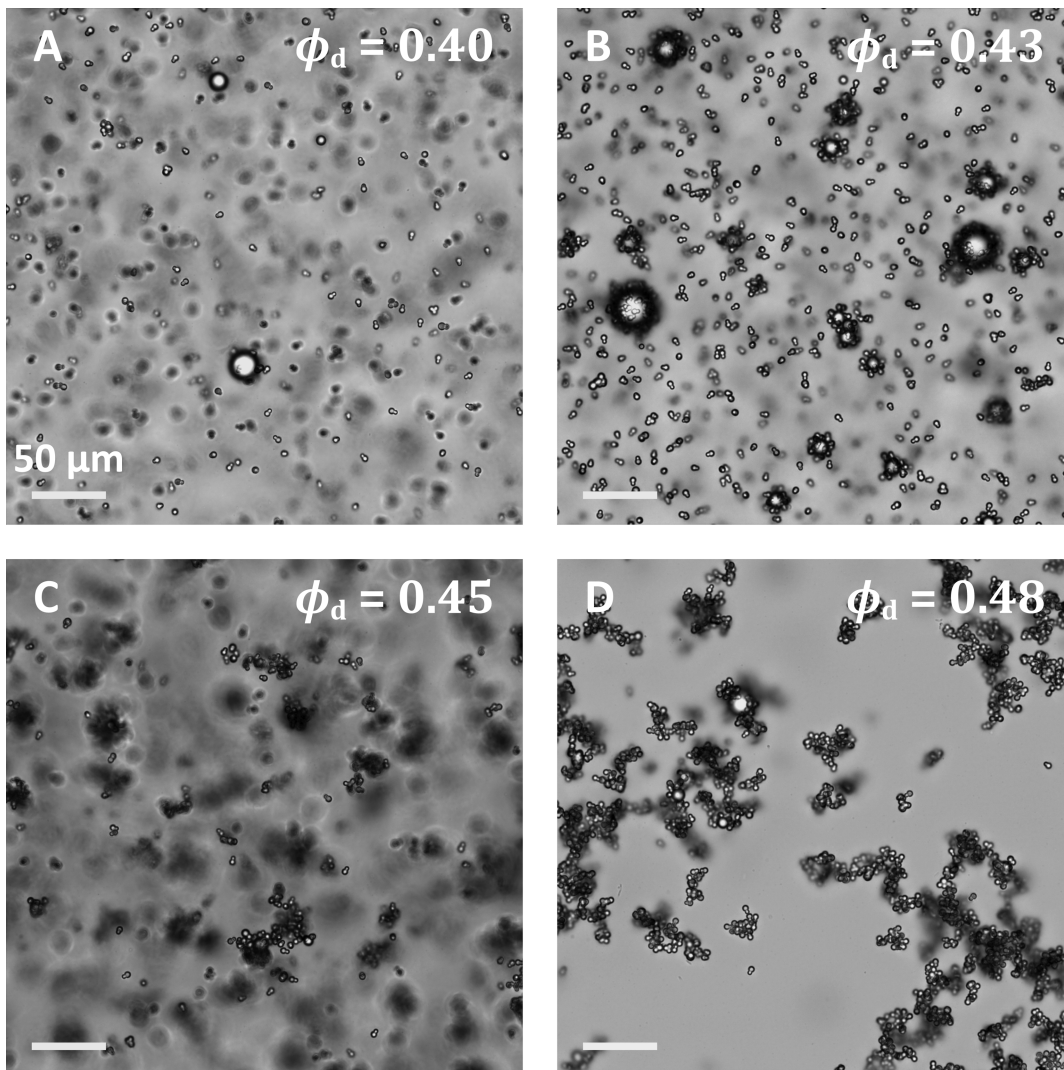


**Figure 3.** Optical microscopy images of the encapsulation of microspheres by colloidal dumbbells with one attractive lobe at increasing dextran concentrations. (A) At a depletant concentration of  $\phi_d = 0.40$ , free dumbbells, free microspheres and sporadically small dumbbell clusters and microspheres with a few dumbbells attached are present in solution. (B) With increasing interaction strength, at  $\phi_d = 0.43$ , more dumbbells start to attach to the microspheres. (C) From a depletant concentration of  $\phi_d = 0.45$ , dumbbells start to form (nonspecific) aggregates. (D) At  $\phi_d = 0.48$ , large random aggregates are visible. All images are taken 3 days after sample preparation. The scalebars represent 50  $\mu\text{m}$ .

An estimate of the net interactions between dumbbells and microspheres can be made based on the particle properties from Table 1, the experimental conditions ( $\phi_d = 0.43$  and 30 mM of salt), and using the equations provided in section 2 of the Supporting Information. This calculation results in an attraction between two smooth lobes (blue line in Figure 2A) with a minimum of  $\epsilon_{ss} = -15.2 k_B T$  and a minimum of  $\epsilon_{sm} = -25.2 k_B T$  for the interaction between a dumbbell's smooth lobe and a microsphere with the ideal radius of  $R_m = 4.83 \mu\text{m}$  (dashed yellow line in Figure 2A). The ratio between these minima equals  $\alpha = \epsilon_{sm}/\epsilon_{ss} = 1.66$ . The gray markers in Figure 2B show how  $\alpha$  develops with microsphere size. For microsphere diameters of  $>16 \mu\text{m}$ , this difference is at least 75% and it goes asymptotically to a value of  $\alpha = 2$  (the interaction between a sphere and a flat wall) for  $R \rightarrow \infty$ .

However, the calculated attraction strengths of  $-15.2 k_B T$  and  $-25.2 k_B T$  do not agree well with experimental observations. Calculating the lifetime of such contacts using Kramers' approach<sup>1,19</sup> results in lifetimes on the order of respectively  $10^6$  and  $10^8$  s, meaning that dumbbell particles

would appear irreversibly stuck on experimental time scales. Yet, in experiments, dumbbells were found to occasionally detach from the microspheres (Figure 5A), and interactions between dumbbells were much more dynamic, with observed lifetimes in a range of  $\tau = 23$  to 268 s (Figure 5B), corresponding to Kramers' escape times for a much more reasonable attractive smooth-smooth potential between  $-6$  and  $-9 k_B T$ . Using  $\alpha = 1.66$  to keep the theoretical ratio, the energy minimum for a smooth-microsphere bond ranges between  $-10$  and  $-15 k_B T$ , resulting in escape times between 468 s and 3 h, which would indeed be consistent with the occasional observation of an unbinding event in experiments.

There is a significant discrepancy between the calculated and observed attraction strength, indicating that a superposition of the depletion attraction and electrostatic repulsion can only provide an approximate description of the interaction potential between the particles. Contributing to this discrepancy is the uncertainty in the surface potential  $\Psi$ , for especially the dumbbell particles, on which the electrostatic repulsion heavily depends ( $\propto \Psi^2$ ). While the particles are sterically stabilized by

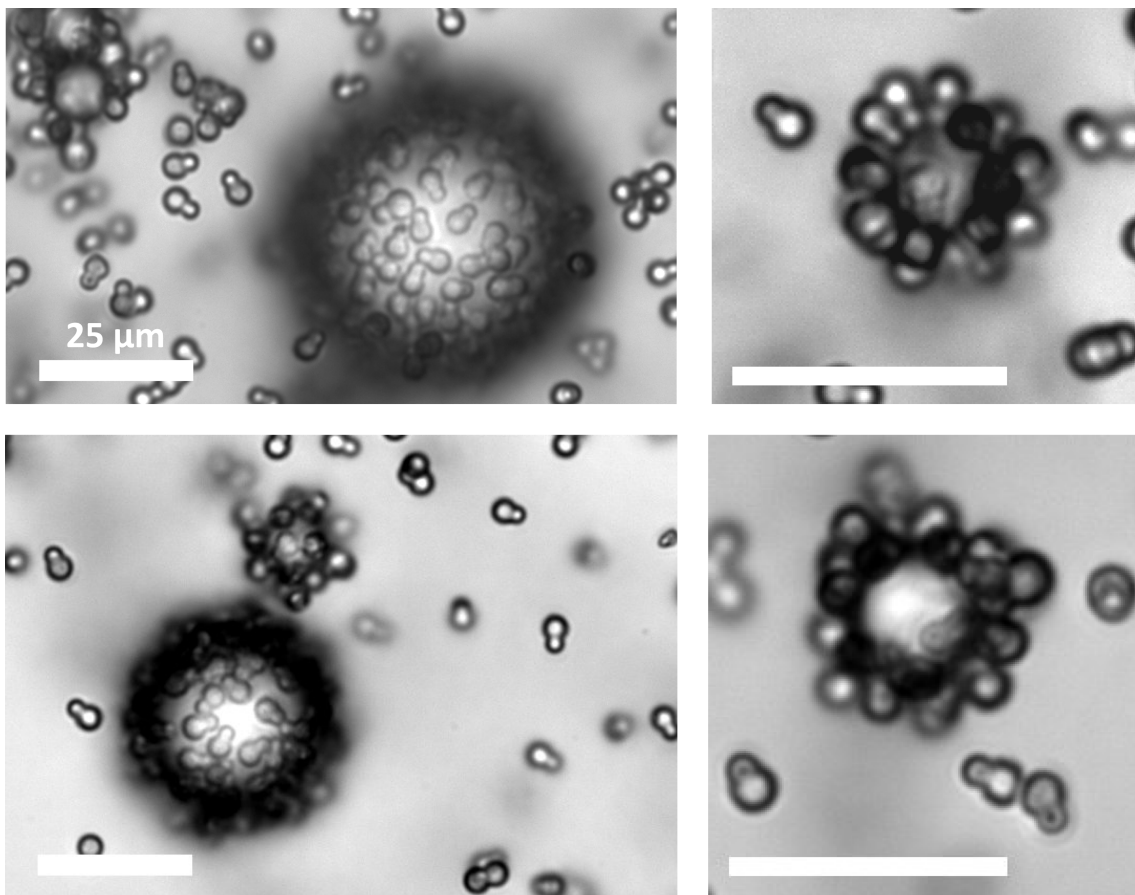


**Figure 4.** Optical microscopy images of encapsulated microspheres at  $\phi_d = 0.43$ . In the left column the sizes of the microspheres equal 39.8 and  $2 \times 10 \mu\text{m}$  (above) and 25.5 and 9.4  $\mu\text{m}$  (below). The microspheres in the right column are approximately 11.0 and 12.8  $\mu\text{m}$ . For small microspheres (8–13  $\mu\text{m}$ ), dumbbells specifically attach with their smooth lobe on the microsphere. For larger microspheres, however, dumbbells appear to lie flat on the surface with both their smooth and rough lobe attached. The scalebars equal 25  $\mu\text{m}$ .

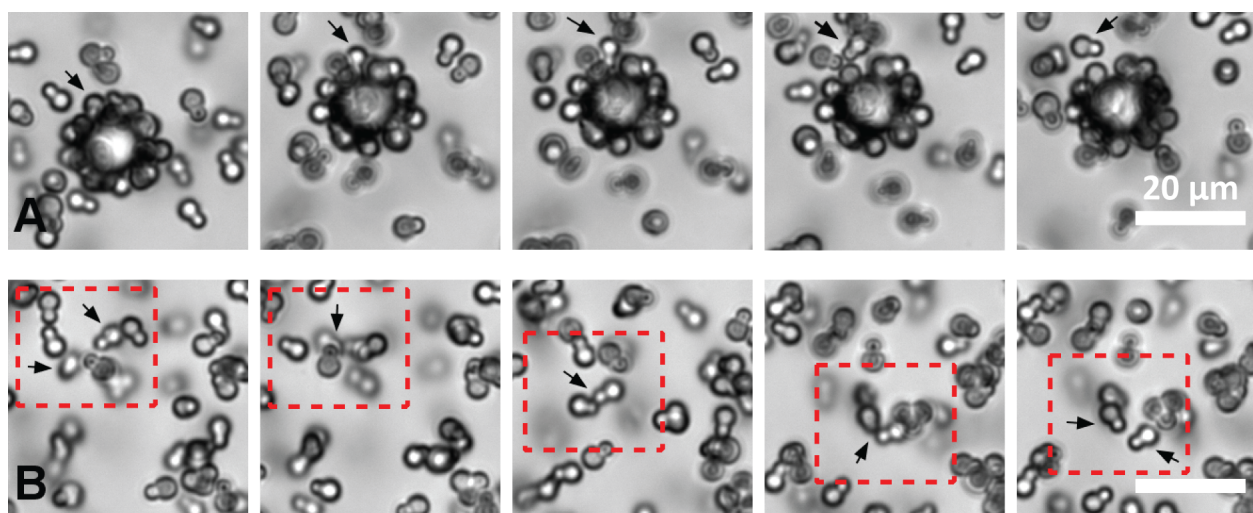


**Figure 5.** (A) Spontaneous unbinding of a colloidal dumbbell from a microsphere in time. (B) Binding and unbinding of a pair of dumbbells in time. A single arrow indicates that the two dumbbells are bound. In this event, a lifetime of  $\tau = 268$  s was observed. Both scalebars represent 20  $\mu\text{m}$ ,  $\phi_d = 0.43$ .

poly(vinyl alcohol) to prevent van der Waals interactions, it is likely that the “softness” of this layer also contributes to the net interaction. Partial interpenetration of the depletant polymer and this adsorbed polymer layer is known to reduce the strength of the depletion attraction.<sup>20</sup>

**Encapsulation in Simulations.** We performed comparative Monte Carlo (MC) simulations to simulate the effect of interaction strength on the coverage of the microsphere. The simulation conditions were chosen such to closely match the experimental values. The size ratio between the rough ( $\sigma_r$ ) and

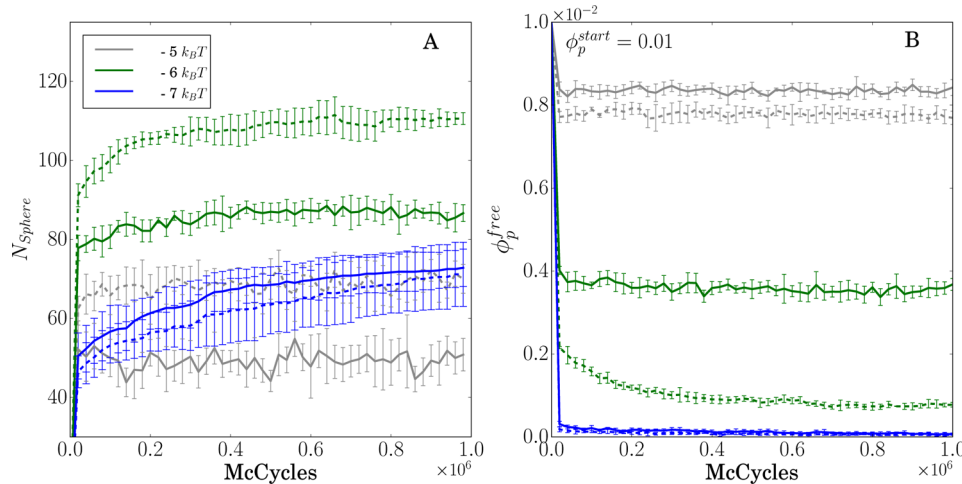


**Figure 6.** (A) Number of attached dumbbells to a single microsphere for simulations with an interaction between the smooth lobes of the dumbbells of either  $-5 \text{ } k_{\text{B}}T$  (gray),  $-6 \text{ } k_{\text{B}}T$  (green), or  $-7 \text{ } k_{\text{B}}T$  (blue) at a volume fraction  $\phi_p = 0.01$ . The dashed lines represent simulations with an additional interaction of  $\gamma\epsilon = -2 \text{ } k_{\text{B}}T$  introduced between the rough lobes of the dumbbells. (B) The decrease in volume fraction of free particles. Visual representations of the final structures are shown in Figure 7.

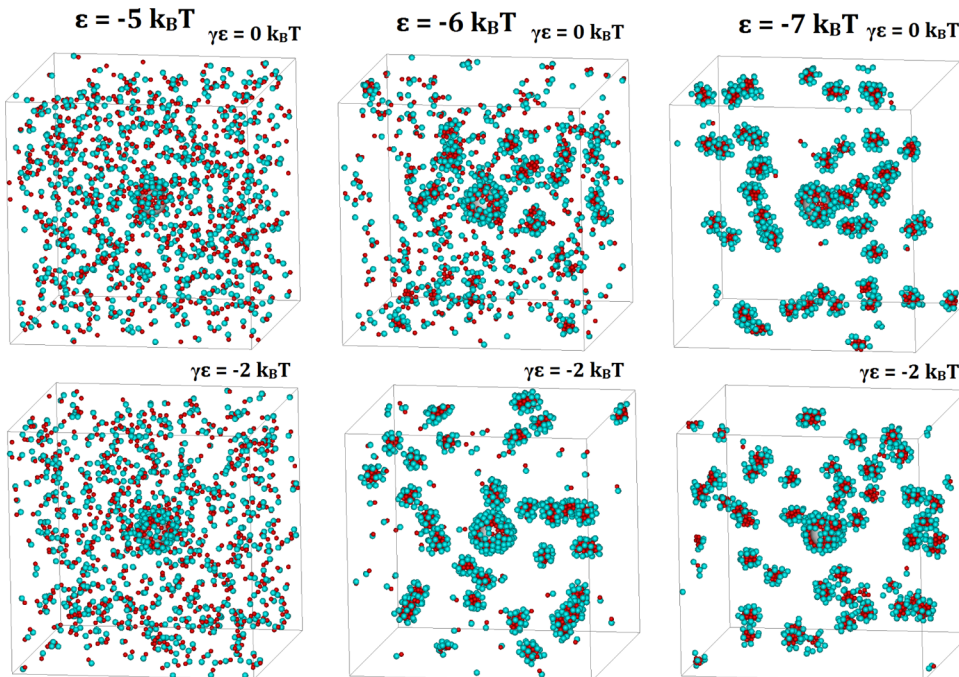


**Figure 7.** Visual representation of MC configurations at three different smooth–smooth interaction energies  $\epsilon$  (columns) and an additional rough–rough attraction  $\gamma\epsilon$  (rows). The simulation conditions are inset in each frame.

smooth ( $\sigma_s$ ) lobes of the dumbbell was set as  $q = \frac{\sigma_r}{\sigma_s} = 1.334$  and the diameter of the microsphere was set at  $\sigma_m = 6.0\sigma_s$ , corresponding to the size of the ideal sphere. The interaction range is set to  $\Delta = 0.024\sigma_s$ , corresponding to the interaction range of  $2r_g = 38 \text{ nm}$  in the experimental system. Simulations were carried out at a dumbbell volume fraction of  $\phi_p = 0.01$  with a fixed microsphere in the center of the simulation box and a potential well depth for the smooth–smooth interaction between two dumbbells of  $\epsilon = -5, -6$  and  $-7 \text{ } k_{\text{B}}T$ . The corresponding attractive potentials between the microsphere and the smooth lobe of a dumbbell were  $\alpha\epsilon = -8.3, -10.0$ , and  $-11.6 \text{ } k_{\text{B}}T$  respectively ( $\alpha = 1.66$ ).

With the rough lobes of the dumbbells acting as hard objects ( $\gamma\epsilon = 0 \text{ } k_{\text{B}}T$ ), simulations were found to converge to a number

of bound dumbbells ( $N_{\text{Sphere}}$ ) from 50 to 87 for  $-5$  and  $-6 \text{ } k_{\text{B}}T$ , respectively (the solid lines in Figure 6A). Yet, with a small additional interaction of  $\gamma\epsilon = -2 \text{ } k_{\text{B}}T$  between the rough lobes of the dumbbells,  $N_{\text{Sphere}}$  converged to approximately 70 and 110 at the same two interaction strengths (dashed lines in Figure 6A).

The volume fraction of free dumbbells started to decrease rapidly due to the formation of micelle-like dumbbell clusters with increasing attraction between the dumbbells (Figures 6B and 7). For an interaction strength of  $-7 \text{ } k_{\text{B}}T$ , this formation of micelle-like structures results in a very low volume fraction of free dumbbells (Figure 6B) and a lower coverage of the microsphere of  $N_{\text{Sphere}} \approx 70$  for both  $\gamma\epsilon = 0$  and  $-2 \text{ } k_{\text{B}}T$ , as was

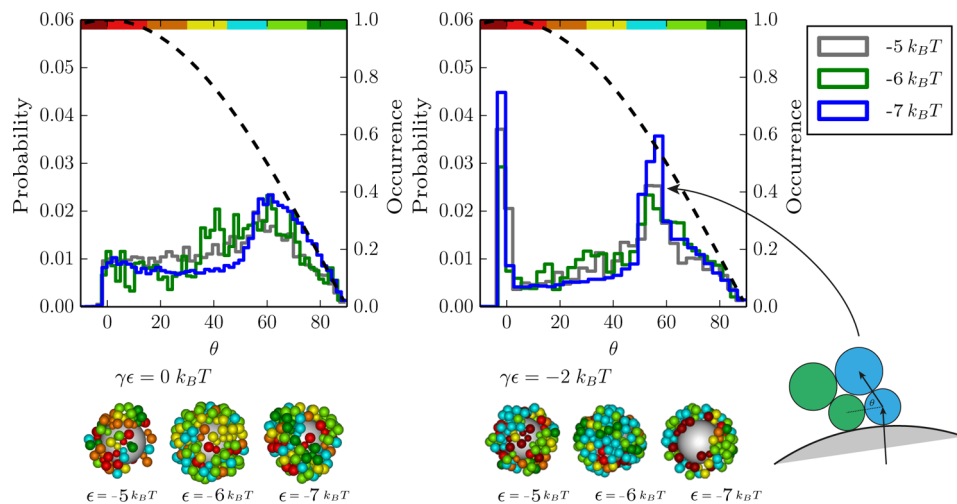


**Figure 8.** 3D angle distribution of dumbbells bound to a microsphere. The interaction energy between the rough lobes of the dumbbells equal  $\gamma\epsilon = 0$   $k_B T$  (left graph) and  $\gamma\epsilon = -2$   $k_B T$  (right graph) at a volume fraction of  $\phi_p = 0.01$ . The angle between a vector and a plane in 3D follows a cosine distribution (represented by the dotted line) due to the increasing number of possible configurations with decreasing  $\theta$ .<sup>21</sup> The probability distribution is not scaled for this difference in angle occurrences. The strong peak emerging at  $\sim 60^\circ$  for  $-2$   $k_B T$  rough–rough attraction corresponds to the orientation of the blue dumbbell in the inset schematic.

verified with extended simulations (up to  $1.8 \times 10^6$  MC cycles) shown in Figure S2.

These results show that in our simulations, an attractive potential of approximately  $-6$   $k_B T$  maximizes the microsphere coverage. While the introduction of an attraction on the rough lobes increases the coverage, full coverage ( $N_{\text{Sphere}} = 132$  to 140) was not achieved.

Additionally, we analyzed the particle orientations with respect to the microsphere surface, finding a gradual distribution with the majority of dumbbells oriented perpendicularly to the microsphere surface and with a small fraction of dumbbells parallel to the surface (Figure 8). Upon introducing an attraction for the rough lobes ( $\gamma\epsilon = -2$   $k_B T$ ), two distinct orientations emerge: one smaller peak at  $\sim 0^\circ$ , representing dumbbells parallel to the surface, i.e., attaching with both their smooth and their rough lobe to the microsphere, and another larger peak at  $\sim 60^\circ$ , corresponding to dumbbells attached with their smooth lobe to the template microsphere and with their rough lobe on the smooth lobe of an adjacent dumbbell. While this extra bond makes this conformation energetically more favorable, it nevertheless frustrates optimal coverage of the microsphere surface. In simulations with larger microspheres ( $\sigma_m = 15.5\sigma_s$  and  $\alpha = 1.80$ ) the  $0^\circ$  orientation occurs more frequently than the  $60^\circ$  orientation since, just like in the experiments, a larger fraction of dumbbells attaches flat to the surface of the larger template microspheres.

**Steric Stabilization by Dumbbell Encapsulation.** Evidently, templated self-assembly of rough–smooth dumbbells on a microsphere surface does not lead to full coverage of the microsphere. This result was also found in the simulations by Munaò et al.<sup>7</sup> as well as in our own computational experiments. To verify that this is inherent to the shape of the dumbbells and not caused by some other experimental condition, we investigated encapsulation of microspheres by spherical particles as a control experiment. In a similar study, where spherical particles attach on the inside of a curved surface by depletion, Meng et al. showed the spherical particles form branched, ribbon-like domains.<sup>22</sup> Keeping the experimental conditions similar to the experiments with dumbbells, spherical

particles (with a radius of  $488 \pm 13$  nm, Table 1) were kept at a volume fraction of  $\phi_p = 1\%$ , microspheres at  $\phi_m = 0.03\%$  and the salt concentration at 30 mM, while the depletant concentration was varied to tune the interaction. Optical microscopy images of these encapsulation experiments with spherical particles are included in the Supporting Information, Figures S3 and S4.

Due to the smaller size and higher zeta potential of the spherical particles, a higher depletant concentration was required to encapsulate the microspheres: the small spheres start attaching to the microspheres at  $\phi_d = 0.45$  and full coverage of the microsphere surface is achieved at  $\phi_d = 0.50$ . At this depletant concentration, multiple layers of small particles on micropshere surfaces were locally observed, but no bulk clustering of small particles.

Just like the dumbbell system, the encapsulation by small particles appears dynamic; particles were found to attach and detach from the microsphere surface. Binding and unbinding events are observed, as well as particles moving over the layer of small particles in a “hopping” manner. The bond lifetimes observed for the spheres are similar to the dumbbell system and using Kramers’ approach in the same way as was done for the dumbbells in this and previous work<sup>1</sup> resulted in a comparable attraction of around  $-7$   $k_B T$ . Besides binding and unbinding of particles, rearrangement of particles to increase the number of contacts with neighboring particles occurred as well. This control experiment shows that spherical particles can, under the same conditions, completely encapsulate a template microsphere. The incomplete coverage observed in encapsulation with dumbbells must therefore be caused by the geometry and Janus-like properties of the dumbbells.

Another striking difference between the microspheres encapsulated by dumbbells and spherical particles is that, in the case of spheres, multiple layers of spheres are formed on the microsphere surface and all microspheres are aggregated into clusters (Figure S3), while those encapsulated by dumbbells were primarily free in solution, with aggregates larger than an occasional dimer being only sporadically observed (see for instance Figures 3 and 4). These results demonstrate that microspheres encapsulated with rough–smooth dumbbells are

to some degree “sterically” stabilized by the rough lobes of the dumbbells on their surface, while a surface covered by smooth microspheres does not provide such stabilization. This enhanced stability was quantified by analyzing the distribution of clusters in samples with a higher  $\phi_m$  of 0.1%, comparing samples without depletant to samples with  $\phi_d \approx 0.45$  and either only microspheres or microspheres combined with spheres or dumbbells. Since diffusion of microspheres is slow, samples were left to equilibrate for 3 weeks before comparing the fraction of particles existing as free particles  $\eta_{\text{free}}$  in each sample (Figure 9). This figure shows that the presence of depletant

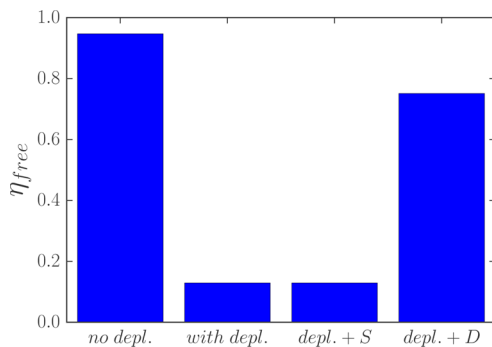


**Figure 9.** Fraction of microspheres existing as free particles  $\eta_{\text{free}}$  in samples with microspheres and without depletant (no depl.) and with depletant (with depl.) and spheres (depl. + S) or dumbbells (depl. + D), showing that encapsulation by dumbbells greatly reduces depletion driven aggregation of microspheres.

causes severe microsphere aggregation, also in the presence of smaller spheres, which is largely prevented by encapsulation with dumbbells.

Since our simulations only contained single microsphere, this stabilization of the microspheres could not be verified with these simulations, but a similar effect was observed in the simulations by Munaò et al.,<sup>7</sup> where the spherical particles were found to aggregate, in this case bridged by the attractive lobes of the dumbbells, in situations with insufficient stabilization by the nonattractive lobes. Such a system of microspheres sterically stabilized by dumbbell particles is reminiscent of simulation experiments performed by Luiken and Bolhuis,<sup>23</sup> where spherical colloids with a square-well attraction are stabilized by penetrable hard spheres tethered to their surface. Luiken and Bolhuis provide an expression to find conditions where the second virial coefficient  $B_2$  equals 0 for their system. Due to the dense coverage by impenetrable hard spheres in the system studied here, an exact value of  $B_2$  cannot be calculated. However, the rough lobes of the dumbbells attached to each microsphere evidently provide a similar means of stabilization, suggesting that also in this situation there is a second virial coefficient  $B_2 \geq 0$ .

**Kinetic Modeling.** Based on thermodynamic considerations, the particles are expected to first completely cover the microsphere surface before forming micelle-like clusters in the bulk at any attractive potential, because they not only bind to the microsphere more strongly than to each other but also because they can additionally bind to up to six other dumbbells on the microsphere surface, resulting in a  $(3 + \alpha)\epsilon$  binding energy per dumbbell, while they only have up to 5 neighbors ( $2.5\epsilon$ ) binding energy in micelles.<sup>1</sup> Likewise, in a molecular system of surfactants, the interface is also completely covered before micelles start to form. This complete coverage of the

microsphere surface is not observed in the experiments, and simulations presented here and the optimal microsphere coverage around  $-6 k_B T$  must therefore originate from the kinetic properties of the system. In order to confirm this, a kinetic model was proposed to relate the microsphere coverage and the concentration of free dumbbells and micelle-like clusters to the attractive potential:



where  $N_{\text{Sphere}}$ ,  $N_{\text{free}}$ , and  $N_{\text{micelle}}$  respectively represent the number of dumbbell particles bound to the microsphere, free in the bulk and present in micelles.  $k_{a,\text{sphere}}$  and  $k_{d,\text{sphere}}$  are the rate coefficients of a dumbbell's adsorption to and desorption from the microsphere.  $k_{a,\text{micelle}}$  and  $k_{d,\text{micelle}}$  are the rate coefficients of a dumbbell's adsorption to and desorption from a micelle-like cluster.

The adsorption rate of a dumbbell to the microsphere is set equivalent to the collision rate of dumbbells in the bulk with the microsphere, times the probability that the dumbbells stick to the microsphere. The collision rate depends on the average time a dumbbell particle has to travel before colliding with the microsphere  $\tau_{\text{stick}}$  while the sticking probability  $p_{\text{stick}}$  depends on the degree of coverage of the microsphere, i.e., the number of bound dumbbells. The desorption rate of dumbbells from the microsphere depends on the escape rate from the square-well potential between a microsphere and a dumbbell (with energy  $-\alpha\epsilon$ ). In summary, for the number of dumbbells onto the microsphere, this becomes

$$\tau_{\text{stick}} = \frac{1}{6D_0} \left( \frac{3(V_{\text{box}} + V_{\text{microsphere}})}{8\pi} \right)^{2/3} \quad (6)$$

$$p_{\text{stick}} = 1 - \frac{N_{\text{Sphere}}}{N_{\text{max}}} \quad (7)$$

$$\tau_{\text{escape}} = \frac{\Delta^2}{D_0} e^{-\alpha\epsilon/k_B T} \quad (8)$$

$$\frac{dN_{\text{Sphere}}}{dt} = k_{a,\text{sphere}} N_{\text{free}} - k_{d,\text{sphere}} N_{\text{Sphere}} \quad (9)$$

$$= \frac{p_{\text{stick}}}{\tau_{\text{stick}}} N_{\text{free}} - \frac{N_{\text{Sphere}}}{\tau_{\text{escape}}} \quad (10)$$

where  $D_0$  is the (perpendicular) translational diffusion coefficient of a dumbbell according to the Stokes–Einstein relation,  $N_{\text{max}}$  is the maximum number of dumbbells that fit on a microsphere (set to 136), and the escape time  $\tau_{\text{escape}}$  from a square-well potential is approximated as the characteristic inverse attempt frequency multiplied by the Arrhenius factor.<sup>24</sup> Note that the system volume  $V_{\text{box}}$  appears in this expression because the current model considers only a single microsphere. In a more general case, with multiple microspheres per volume, quantities would depend on the concentration  $N/V$  instead.

Besides attachment to the microsphere, the particles also form micelle-like clusters. The fraction of dumbbells present in micelle-like clusters depends on the formation rate of such clusters and the escape rate of dumbbells from existing clusters. The rates of dumbbells sticking to and escaping from such clusters are hard to estimate, because both parameters heavily depend on the structure of the cluster and because its contacts

can be broken sequentially, making both rates depend on unknown pathways. As an approximation, the formation rate was set to depend on the (approximate) average time a dumbbell can travel before colliding with another dumbbell or micelle-like cluster, introducing a probability  $0 < f < 1$  of successfully attaching to a micelle, since its outside is primarily shielded by rough lobes. In the escape rate, sequential breaking of bonds leads to an addition of escape times, while the time to break multiple bonds simultaneously increases exponentially with the number of bonds, making simultaneous bond breaking decisive in determining the escape rate from clusters.

$$k_{a,\text{micelle}} = 6fD_0 \left( \frac{N_{\text{free}} + \frac{1}{n_c} N_{\text{micelle}}}{V_{\text{box}}} \right)^{2/3} \quad (11)$$

$$k_{d,\text{micelle}} = \frac{1}{\tau_{\text{escape},nbonds}} = \frac{D_0}{\Delta^2} e^{n_b \epsilon} \quad (12)$$

$$\frac{dN_{\text{micelle}}}{dt} = k_{a,\text{micelle}} N_{\text{free}} - k_{d,\text{micelle}} N_{\text{micelle}} \quad (13)$$

where  $f$  (the probability of a dumbbell successfully binding to a micelle) is set to 0.05 due to screening by rough lobes,  $n_c$  is the average number of dumbbells in a micelle-like cluster ( $\sim 10$ ), and  $n_b$  is the number of bonds that need to be broken simultaneously to remove a dumbbell from a cluster (set to 2). This number is rationalized by considering that a particle bound to 4 or more particles (5 on average in micelle-like clusters)<sup>1</sup> can only move by initially breaking 2 bonds simultaneously (approximated by escaping a well of twice the depth). This takes exponentially more time and is thus considered to be the rate limiting step.

Using this model,  $N_{\text{Sphere}}$ ,  $N_{\text{free}}$ , and  $N_{\text{micelle}}$  can be obtained as a function of the degree of attraction  $\epsilon$  by setting eqs 10 and 13 equal to 0 and imposing  $N_{\text{total}} = N_{\text{Sphere}} + N_{\text{free}} + N_{\text{micelle}}$ . Note that by doing so the equilibrium state of the system does no longer depends on the system dynamics (diffusion coefficients), as it should, but is established based on the binding energies and probabilities and the concentrations of the species involved. The total number of dumbbells  $N_{\text{total}}$  is set to 800, the number used in the simulations. The resulting number of dumbbells attached to the microsphere  $N_{\text{Sphere}}$ , as well as the number present in micelles  $N_{\text{micelle}}$  and free dumbbells  $N_{\text{free}}$  are plotted as a function of  $\epsilon$  in Figure 10.

Using the chosen parameters, the kinetic model agrees well with the observations from both simulations and experiments while making as little assumptions as possible about the formation and dissociation pathways involved. Had the escape rate from micelles been lower (e.g.,  $n_b = 1$ , so  $n_b < \alpha$ ), the system would always converge to optimal coverage with increasing attraction strength, while extended simulations (Figure S2) show that  $N_{\text{Sphere}}$  converges to a lower number for  $\epsilon = -7 k_B T$  than for  $\epsilon = -6 k_B T$ . The rough lobes on the outside of the micelle-like clusters limit such clusters to finite size by preventing new dumbbells from attaching. The introduction of this screening of factor  $f = 0.05$  is not necessary to describe the competition between encapsulation and micelle formation qualitatively but allows for the model to quantitatively better agree with the observations from experiments and simulations.

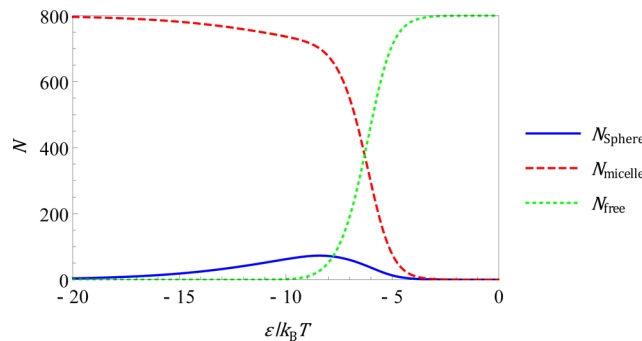


**Figure 10.** Number of dumbbells attached to the microsphere ( $N_{\text{Sphere}}$ , solid blue line), in micelles ( $N_{\text{micelle}}$ , dashed red line) and free in solution ( $N_{\text{free}}$ , dotted green line) as a function of the attraction strength  $\epsilon$  according to our kinetic model, showing a maximum of  $N_{\text{Sphere}}$  around  $\epsilon \approx -6 k_B T$ .

## CONCLUSIONS

In this paper we investigated the encapsulation of microspheres by rough-smooth dumbbells through depletion interaction. With increasing depletant concentration, the dumbbells were either free in solution or specifically bound with their smooth lobes to the microspheres and to each other, forming micelle like clusters. At even higher depletant concentrations, all particles were nonspecifically bound to the microspheres and each other, forming random aggregates.

In the case of specifically bound dumbbells, the encapsulation depends strongly on the curvature of the microsphere surface; dumbbells on large microspheres primarily lie flat, binding with both their smooth and rough lobe to the surface, while for smaller microspheres, a majority of dumbbells bind with only their smooth lobe, orienting perpendicular to the surface.

Based on the lifetime of pairs of dumbbells, we estimated the smooth–smooth attraction in the experimental system to be  $-6$  to  $-9 k_B T$ , which corresponds to a smooth–microsphere attraction of  $-10$  to  $-15 k_B T$  based on the larger overlap volume and different surface potential between a dumbbell and a microsphere. The occasionally observed unbinding of a dumbbell from a microsphere is indeed expected for such a value of the potential minimum.

In addition to the depletion experiments, we performed Monte Carlo simulations mimicking the experimental conditions. For the smaller microspheres, the simulation results show the same preferred particle orientation perpendicular to the surface that was also found in the depletion experiments. Also in simulations, this preference is lost for larger microspheres.

Introducing an attractive potential to the rough lobes of the dumbbells in the simulations increased the coverage of the microsphere surface. Furthermore, it led to the emergence of two distinct dumbbell orientations; one parallel to the microsphere surface and the other at an angle of approximately  $60^\circ$ . The parallel orientation represented dumbbells binding with both their lobes to the microsphere. This orientation was most predominant on the larger microspheres.

While the thermodynamic ground state of this system is expected to be a microsphere fully covered with close-packed dumbbells, complete coverage was observed in neither experiments nor simulations. However, in a control experiment with smooth, spherical particles instead of dumbbells, full coverage of the microspheres was observed. This observation suggests that the shape of the dumbbell kinetically frustrates

optimal coverage of the microspheres. A simple kinetic model supports experimental evidence that maximal coverage of the microspheres is achieved at moderate dumbbell–dumbbell attraction, while for stronger attraction, more dumbbells end up forming micelle-like clusters, a process competing with microsphere encapsulation.

Additionally, in the encapsulation experiments with smooth, spherical particles, the smaller particles locally formed multiple layers on the microsphere surface. Moreover, large aggregates of covered microspheres were observed. Conversely, in the encapsulation experiments with dumbbells, the coverage was limited to a single layer and aggregates of microspheres were only sporadically observed. This confirms that, even though the microspheres are not completely covered, the rough lobes of the dumbbells on their surface still supply a significant degree of “steric” stabilization, providing stabilization by aggregation.

## ■ ASSOCIATED CONTENT

### S Supporting Information

The Supporting Information is available free of charge on the ACS Publications website at DOI: [10.1021/acs.langmuir.7b00014](https://doi.org/10.1021/acs.langmuir.7b00014).

Detailed description of the particle synthesis and the calculation of the interaction potentials, a graph of the extended MC simulations at  $-7 k_B T$ , and the optical microscopy results of the encapsulation experiments with spherical particles ([PDF](#))

## ■ AUTHOR INFORMATION

### Corresponding Author

\*E-mail: [w.k.kegel@uu.nl](mailto:w.k.kegel@uu.nl). Phone: +31 (0)30 253 2873.

### ORCID

Joost R. Wolters: [0000-0001-5000-6281](https://orcid.org/0000-0001-5000-6281)

### Author Contributions

<sup>§</sup>J.R.W. and J.E.V. contributed equally.

### Notes

The authors declare no competing financial interest.

## ■ ACKNOWLEDGMENTS

The authors acknowledge Daniela Kraft for useful discussions and Sonja Castillo for taking the SEM images. This work was funded by The Netherlands Organization for Scientific Research (NWO) through a TOP-Go Grant (J.R.W. and W.K.K.) and the FOM research program (G.A.)

## ■ REFERENCES

- (1) Kraft, D. J.; Ni, R.; Smallenburg, F.; Hermes, M.; Yoon, K.; Weitz, D. A.; van Blaaderen, A.; Groenewold, J.; Dijkstra, M.; Kegel, W. K. Surface roughness directed self-assembly of patchy particles into colloidal micelles. *Proc. Natl. Acad. Sci. U. S. A.* **2012**, *109*, 10787–10792.
- (2) Zhang, Z.; Glotzer, S. C. Self-assembly of patchy particles. *Nano Lett.* **2004**, *4*, 1407–1413.
- (3) Chen, T.; Zhang, Z.; Glotzer, S. C. A precise packing sequence for self-assembled convex structures. *Proc. Natl. Acad. Sci. U. S. A.* **2007**, *104*, 717–722.
- (4) Wilber, A.; Doye, J.; Louis, A.; Noya, E.; Miller, M.; Wong, P. Reversible self-assembly of patchy particles into monodisperse icosahedral clusters. *J. Chem. Phys.* **2007**, *127*, 085106.
- (5) den Otter, W.; Renes, M.; Briels, W. Self-assembly of three-legged patchy particles into polyhedral cages. *J. Phys.: Condens. Matter* **2010**, *22*, 104103.
- (6) Williamson, A. J.; Wilber, A. W.; Doye, J. P. K.; Louis, A. A. Templated self-assembly of patchy particles. *Soft Matter* **2011**, *7*, 3423–3431.
- (7) Munao, G.; Costa, D.; Prestipino, S.; Caccamo, C. Encapsulation of spherical nanoparticles by colloidal dimers. *Phys. Chem. Chem. Phys.* **2016**, *18*, 24922–24930.
- (8) Hong, J.; Hong, C.; Shim, S. Synthesis of polystyrene microspheres by dispersion polymerization using poly(vinyl alcohol) as a steric stabilizer in aqueous alcohol media. *Colloids Surf., A* **2007**, *302*, 225–233.
- (9) Kim, J.-W.; Larsen, R. J.; Weitz, D. A. Synthesis of Nonspherical Colloidal Particles with Anisotropic Properties. *J. Am. Chem. Soc.* **2006**, *128*, 14374–14377.
- (10) Badaire, S.; Cottin-Bizonne, C.; Woody, J. W.; Yang, A.; Stroock, A. D. Shape selectivity in the assembly of lithographically designed colloidal particles. *J. Am. Chem. Soc.* **2007**, *129*, 40–41.
- (11) Wolters, J. R.; Avvisati, G.; Hagemans, F.; Vissers, T.; Kraft, D. J.; Dijkstra, M.; Kegel, W. K. Self-assembly of “Mickey Mouse” shaped colloids into tube-like structures: experiments and simulations. *Soft Matter* **2015**, *11*, 1067–1077.
- (12) Rasband, W. *ImageJ*; U.S. National Institutes of Health: Bethesda, Maryland, <http://imagej.nih.gov/ij/>.
- (13) Schneider, C. a.; Rasband, W. S.; Eliceiri, K. W. NIH Image to ImageJ: 25 years of image analysis. *Nat. Methods* **2012**, *9*, 671–675.
- (14) Rogers, C. Covering a sphere with spheres. *Mathematika* **1963**, *10*, 157–164.
- (15) Balmer, J. A.; Armes, S. P.; Fowler, P. W.; Tarnai, T.; Gáspár, Z.; Murray, K. A.; Williams, N. S. J. Packing efficiency of small silica particles on large latex particles: a facile route to colloidal nanocomposites. *Langmuir* **2009**, *25*, 5339–5347.
- (16) Noro, M. G.; Frenkel, D. Extended corresponding-states behavior for particles with variable range attractions. *J. Chem. Phys.* **2000**, *113*, 2941–2944.
- (17) Foffi, G.; Sciortino, F. On the possibility of extending the Noro-Frenkel generalized law of correspondent states to nonisotropic patchy interactions. *J. Phys. Chem. B* **2007**, *111*, 9702–9705.
- (18) Hardin, R.; Sloane, N.; Smith, W. Tables of Spherical Codes with Icosahedral Symmetry. published electronically at <http://neilsloane.com/icosahedral.codes/>.
- (19) Kramers, H. A. Brownian motion in a field of force and the diffusion model of chemical reactions. *Physica* **1940**, *7*, 284–304.
- (20) Vincent, B.; Edwards, J.; Emmett, S.; Jones, A. Depletion flocculation in dispersions of sterically-stabilised particles (“soft spheres”). *Colloids Surf.* **1986**, *18*, 261–281.
- (21) Beltman, J.; Marée, A.; de Boer, R. Analysing immune cell migration. *Nat. Rev. Immunol.* **2009**, *9*, 789–798.
- (22) Meng, G.; Paulose, J.; Nelson, D. R.; Manoharan, V. N. Elastic instability of a crystal growing on a curved surface. *Science* **2014**, *343*, 634–637.
- (23) Luiken, J. A.; Bolhuis, P. G. Anisotropic aggregation in a simple model of isotropically polymer-coated nanoparticles. *Phys. Rev. E* **2013**, *88*, 012303.
- (24) Felderhof, B. Escape by diffusion from a square well across a square barrier. *Phys. A (Amsterdam, Neth.)* **2008**, *387*, 39–56.